Deposition, characterization and performance evaluation of ceramic coatings on metallic substrates for supercritical water-cooled reactors

Hui, Rob; Cook, William; Sun, Chunwen; Xie, Yongsong; Yao, Peter; Miles, Jamie; Olive, Robert; Li, Jian; Zheng, Wenyue; Zheng, Lefu

Publisher's version / Version de l'éditeur:
https://doi.org/10.1016/j.surfcoat.2010.12.017
Surface & Coatings Technology, 205, 11, pp. 3512-3519, 2010-12-21

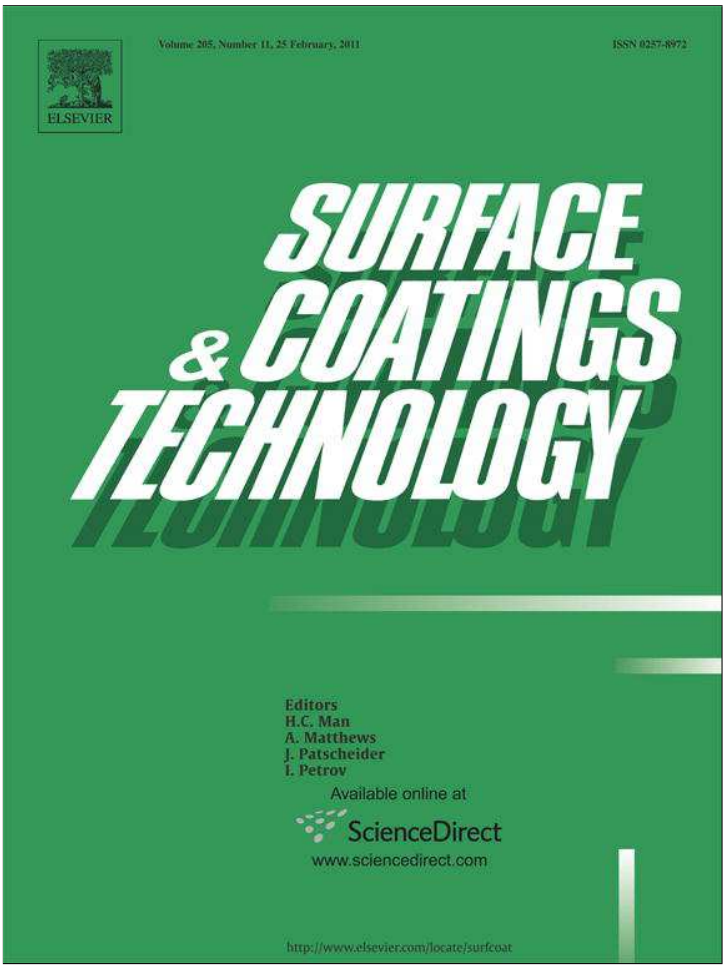

Surface & Coatings Technology 205 (2011) 3512–3519

Contents lists available at ScienceDirect

Surface & Coatings Technology

journal homepage: www.elsevier.com/locate/surfcoat

Deposition, characterization and performance evaluation of ceramic coatings on metallic substrates for supercritical water-cooled reactors

Rob Hui [a,*], William Cook [b], Chunwen Sun [a], Yongsong Xie [a], Peter Yao [a], Jamie Miles [b], Robert Olive [b], Jian Li [c], Wenyue Zheng [c], Lefu Zhang [d]

[a] NRC – Institute for Fuel Cell Innovation, 4250 Wesbrook Mall, Vancouver, BC, Canada, V6T 1W5
[b] Department of Chemical Engineering, University of New Brunswick, Fredericton, New Brunswick, Canada, E3B 5A3
[c] CANMET–Materials Technology Laboratory, Natural Resources Canada, 568 Booth Street Ottawa, Ontario, Canada, K1A 0G1
[d] School of Nuclear Science and Engineering, Shanghai Jiaotong University, No. 800, Dongchuan Road, Minhang, Shanghai 200240, P. R. China

ARTICLE INFO

Article history:
Received 14 September 2010
Accepted in revised form 14 December 2010
Available online 21 December 2010

Keywords:
Ceramic coatings
Supercritical water-cooled reactors (SCWR)
Gen IV
Plasma electrolytic oxidation
Spray pyrolysis
Protective coatings
Corrosion

ABSTRACT

A series of ceramic coatings have been prepared on P91 substrates by spray pyrolysis processes and on Zr–2.5Nb substrates by a plasma electrolytic oxidation process. Preliminary results show that coatings obtained with different solution compositions and procedures can reduce the oxidation weight gain of P91 samples by factors of 2–10 for exposure times up to 500 h in deaerated supercritical water at 500 °C and 25 MPa. Results also show that the weight gain of a P91 sample with an alumina (Al_2O_3) coating is about nine times less than that of uncoated P91 after exposures for 400 h in deaerated supercritical water at 650 °C and 25 MPa. These results indicate that the Al_2O_3 coating shows promising results for preventing oxidation of P91 under supercritical water conditions. The samples with ceramic coatings on Zr–2.5Nb substrates show marginally improved corrosion resistance compared to the bare substrates.

1. Introduction

In recent years, due to the increased need to control worldwide CO_2 emissions, the option of energy production by CO_2-free nuclear fission reactors has become more and more attractive. The Generation IV International Forum (GIF) has selected six innovative concepts for nuclear reactors based on safety and environmental issues [1]. One of the most promising advanced reactor concepts is the supercritical water-cooled reactor (SCWR). Operating above the thermodynamic critical point of water (374 °C, 22.1 MPa), SCWRs offer many advantages compared to current light water reactors (LWRs), such as the use of a single phase coolant with high enthalpy, the elimination of expensive components such as steam generators, dryers, and a low coolant mass inventory resulting in smaller components with much higher thermal efficiency (i.e., up to 50% thermal efficiency vs. about 33% thermal efficiency for LWRs) as well as better fuel usage [2]. The SCWR design fulfils the criteria of economics, safety and sustainability considered in the Generation IV International Forum. Unfortunately, accompanying the increased efficiency, supercritical water at higher operating temperatures and pressures is much more aggressive for in-core and out-core components than the coolant in current water-cooled reactors, especially under oxidizing environments. At high temperature and with increased dissolved oxygen concentrations, a metal or alloy's oxidation rate is significantly enhanced [3].

Typical materials for applications using high-temperature and high-pressure aqueous solutions are ferritic–martensitic (F/M) stainless steels, nickel-based alloys, titanium, tantalum, noble metals or ceramics [4,5]. Although metallic or alloyed materials have the advantages of high mechanical strength and easy fabrication into complex shapes, these materials may be severely attacked under the oxidizing conditions of a SCWR. Ceramic materials known for their good corrosion resistance have been suggested as a suitable material for supercritical water oxidation (SCWO) applications [6]. Hara et al. carried out a screening test of 18 kinds of ceramics and demonstrated that oxide ceramics had better corrosion resistance than non-oxide ceramics in a SCW environment [7]. Boukis et al. measured the corrosion behaviour of various ceramics in a simulated SCWO environment [8]. Their results showed that only a few Al_2O_3- and ZrO_2-based materials did not corrode severely in this very corrosive fluid. In comparison, HIP-BN, B_4C, TiB_2, Y_2O_3 and Y-TZP disintegrated; SiC- and Si_3N_4-based materials showed a large weight loss of up to 90%. One obvious disadvantage of ceramics is that the mechanical strength is usually not sufficient for practical applications. Advanced ceramic coatings combined with an alloy substrate may offer the ideal properties that are suitable for use in a SCWR.

* Corresponding author. Tel.: +1 604 221 3111; fax: +1 604 221 3001.
E-mail address: rob.hui@nrc-cnrc.gc.ca (R. Hui).

0257-8972/$ – see front matter.
doi:10.1016/j.surfcoat.2010.12.017

Table 1
Nominal chemical composition of P91 alloy (wt.%, bal. Fe) [3].

C	Mn	P	S	Si	Ni	Cr	Mo	Cu	N	Cb	Al	V
0.1	0.45	0.009	0.003	0.28	0.21	8.37	0.90	0.17	0.048	0.076	0.022	0.216

Spray pyrolysis deposition (SPD) is a cost-effective process to deposit films on a variety of materials [9]. The process involves atomizing a solution containing soluble salts of the constituent atoms of the desired compound and spraying the droplets onto a heated substrate. The droplets reaching the hot substrate surface undergo pyrolytic decomposition and form a chemical compound. The chemical reactants are selected such that the products, are volatile at the temperature of deposition and thus escape into the vapor phase. The substrate provides the thermal energy for the thermal decomposition and subsequent sintering of the constituent species giving rise to a coherent film. The main advantages of SPD include the simplicity of the apparatus, the low cost of the process and the ease of scalability to larger components. The National Research Council Canada's Institute for Fuel Cell Innovation (NRC-IFCI) has been developing spray pyrolysis techniques for various applications since 2004. Processes for depositing various oxide films have been developed [10]. In this study, dense and well-bonded ceramic oxide layers have been successfully deposited on P91 substrates using spray pyrolysis and were examined in a SCW environment in an autoclave.

Plasma electrolytic oxidation (PEO), also called plasma electrolytic deposition, micro-arc oxidation, pulse plasma anodization or spark anodization, is a novel method to produce hard and corrosion-resistant ceramic coatings on Al, Mg, Ti, Zr and other light metals as well as their alloys [11]. The PEO method utilizes the formation of micro-arc plasma discharges on the surface of the workpiece treated in an electrolytic aqueous solution. The coatings are typically 10–50 μm thick with crystalline or amorphous phases containing oxides of metals in the substrate and electrolyte constituents [12–14]. Properties of this multi-function protective ceramic coating include very high hardness, excellent wear resistance, excellent corrosion resistance, extremely high coating–substrate adhesion, high thermal shock resistance, and dielectric properties. The excellent wear, friction, corrosion, and thermal properties of these coatings are of particular interest in textile machines, aerospace components, oil and gas extraction and refining machinery, and nuclear power plants. In this study, well-bonded zirconia coating without open pores has been successfully formed on Zircaloy substrates using plasma electrolytic oxidation and examined in SCW environments in autoclaves and re-circulating test loops.

2. Experimental

The chemical composition of P91 alloy used as one of the substrate materials has been listed in Table 1 [3]. Commercial P91 plate (American Alloy Steel, Inc.) and Zircaloy bar (Zr–2.5Nb, ATI Wah Chang) were cut into samples with dimensions of 50 mm × 10 mm × 1 mm. Prior to the SPD and PEO treatments, the specimens were polished with 400 grit SiC abrasive paper with a roughness (R_a) value of 1.50 μm, degreased with acetone and then rinsed with deionized water and allowed to air dry.

The spray pyrolysis deposition technique was utilized to deposit a dense coating of metal oxides on the pre-cleaned P91 stainless steel substrates. In the pneumatic spray deposition (PSD) process, a compressed gas was utilized to atomize and spray a precursor solution; in the integrated PSD and electrostatic spray deposition (ESD) process, an electrostatic field and the compressed gas are both applied to atomize and spray a precursor solution.

In order to produce dense coatings for corrosion protection, various experiments were carried out to determine the optimized deposition conditions. Organic solutions containing $Al(NO_3)_3$, $(NH_4)_2Ce(NO_3)_6$ plus tantalum isopropoxide, and $Mg(NO_3)_2$ plus Zr *n*-butoxide *n*-butanol complex were prepared to provide precursors for Al_2O_3, $(Ta_2O_5)_{0.04}(CeO_2)_{0.96}$ and $(MgO)_{0.01}$ $(ZrO_2)_{0.99}$ coatings, respectively. The pH of the $Al(NO_3)_3$ solution was adjusted by $NH_3 \cdot H_2O$. Precursors containing multi-metal elements were prepared according to the stoichiometric ratios desired in the metal oxides. The depositions were carried out with 120 passes of spray and the substrate temperatures were controlled around 380 °C during the deposition with compressive air as spray gas. The as-coated samples were then heated in situ at 600 °C for Al_2O_3 coatings and 650 °C for the others for 30 min in air. The influence of the heat treatment at 600 °C after deposition on the microstructure and property of the substrates has been minimized with such short exposure period. The detailed experiment conditions and the thickness of the coatings obtained are listed in Table 2.

Plasma electrolytic oxidation was utilized to form the ceramic coatings on Zr–2.5Nb substrates as S6 in Table 2. For plasma electrolytic oxidation, an appropriate pulsed power source developed by NRC-IFCI was used for the PEO treatment of the samples. The PEO unit consists of a water-cooled glass electrolyser with a stainless steel liner and a high power electrical source. The stainless steel liner also serves as the counter electrode. The electrolyte solution in this study was an aqueous solution consisting of 14 g/L of sodium silicate (Na_2SiO_3). After the treatment, the coated samples were rinsed with deionized water and dried in air.

The pulse duty ratio is defined as follows:

$$\text{Duty ratio}(D) = \frac{t_{on}}{t_{on} + t_{off}} \times 100\%, \quad (1)$$

where t_{on} is the pulse on-time and t_{off} is the pulse off-time. In this study, the duty ratio of the negative pulse (D_n) was set as 10%; negative pulse voltage U_n was fixed at 50 V; the number of negative pulses was 1, i.e., a cycle of three positive pulses was followed by one negative pulse. The duty ratio of the positive pulse (D_p) and the positive/negative pulse proportion (R) were set to 20% and 3, respectively. At the early stage of this process, a constant current mode was used at an average current density of 0.05 A/cm^2. The

Table 2
Conditions for coating preparation discussed in this work.

Sample ID	Substrate materials	Coating composition	Coating thickness (μm)	Deposition Conditions		
				method	Substrate temperature (°C)	pH of precursor or electrolyte solution
S1	P91	Al_2O_3	5	PSD	600	2
S2	P91	Al_2O_3	5	PSD	600	3.5
S3	P91	$(Ta_2O_5)_{0.04}$ $(CeO_2)_{0.96}$	2.5	PSD	650	N/A
S4	P91	$(MgO)_{0.01}$ $(ZrO_2)_{0.99}$	2.5	PSD	650	N/A
S5	P91	Al_2O_3	5	PSD + ESD	600	2
S6	Zircaloy (Zr–2.5Nb)	ZrO_2	30	PEO	25	12.5

positive pulse voltage U_p was gradually increased with the build-up of the films and it reached 520 V after about 20 min after which a constant voltage was maintained for further oxidation. The total time for PEO treatment was 7 h.

The phase composition of coatings was examined by X-ray powder diffraction (XRD) performed on a Bruker AXS D8 Advance with Cu K_α radiation. The morphology of the surfaces and cross-sections of the coatings were characterized using a scanning electron microscope (SEM, Hitachi S-3500N, Japan). Prior to the SEM examinations, the samples were coated with gold by sputtering to minimize charging effects under SEM imaging conditions. Chemical compositions and elemental distributions were analysed by X-ray energy dispersion spectroscopy (EDS) coupled to the SEM (Oxford, UK).

The flow loop and autoclave testing was carried out collaboratively with the University of New Brunswick and Shanghai Jiao Tong University, respectively. The P91 based samples were mainly tested at University of New Brunswick and the test conditions were 500 °C at 25 MPa (pH ~ 7 at room temperature) with a dissolved oxygen concentration (DO) of less than 20 μg/kg and a water flow rate of 0.2 kg/min. The zirconium-based samples were tested at both UNB and Shanghai JiaoTong University; the test conditions were 500 °C, 25 MPa, DO < 5 ppb, without dissolved hydrogen (DH) in Shanghai and the same conditions as for the P91 samples at UNB. The P91 with Al_2O_3 coating was also tested at Shanghai JiaoTong University under different test conditions which were 650 °C at 25 MPa with a DO content of less than 2 μg/kg, saturated DH at about 1.5 mg/kg and a water flow rate about 0.8 l/h.

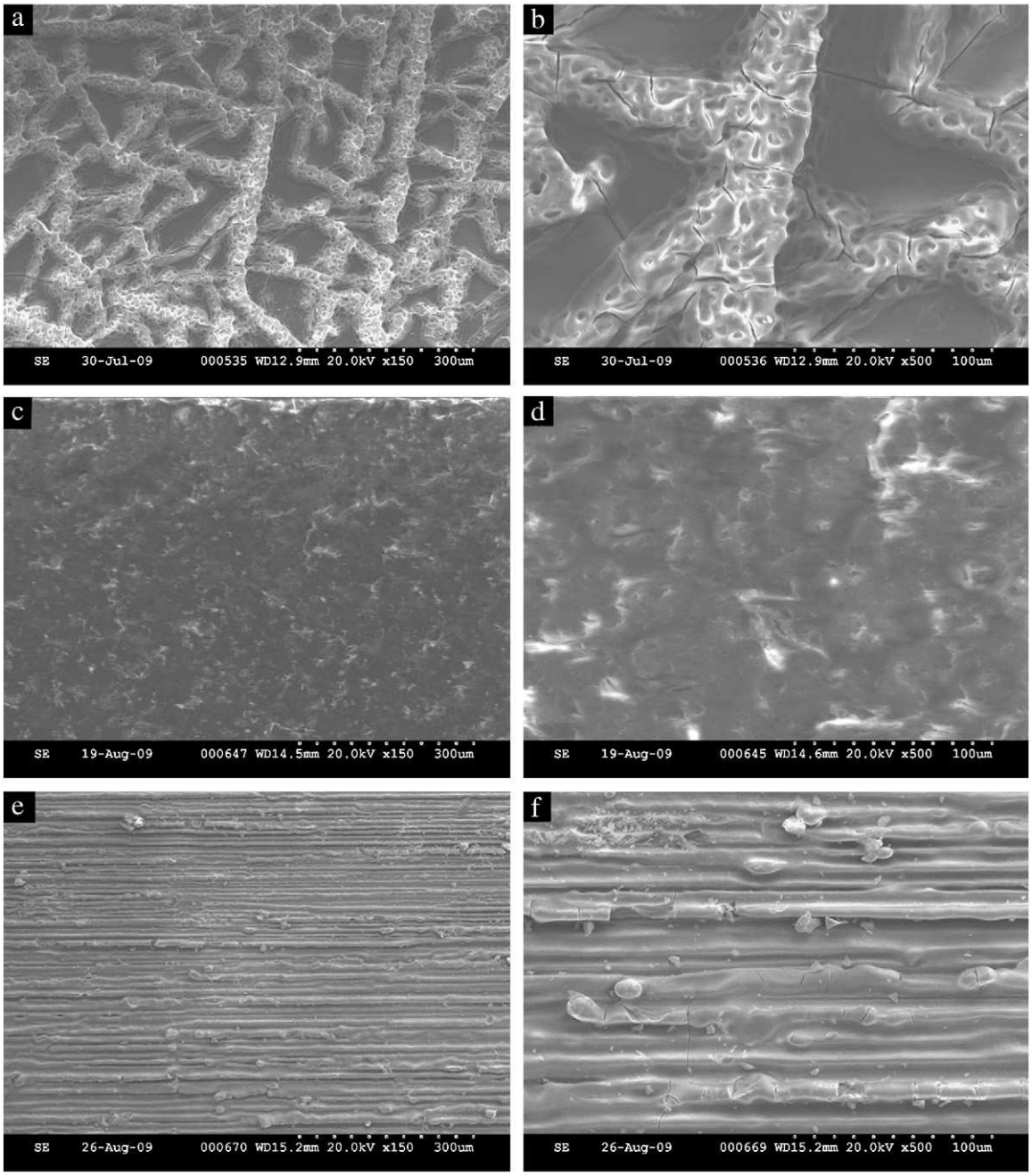

Fig. 1. Surface SEM images of the coatings on P91 prepared by spray pyrolysis: (a, b) S1 – Al_2O_3 (c, d) S2 – Al_2O_3; (e, f) S3 – CeO_2-Ta_2O_5; (g, h) S4 – ZrO_2-MgO; and (i, j) S5 – Al_2O_3. (Note: the grooves in e, f, g, h are the original machining grooves in the substrates. Because the roughness of these substrates was greater than the coating thickness, the coatings replicated the grooves, rather than covering them.)

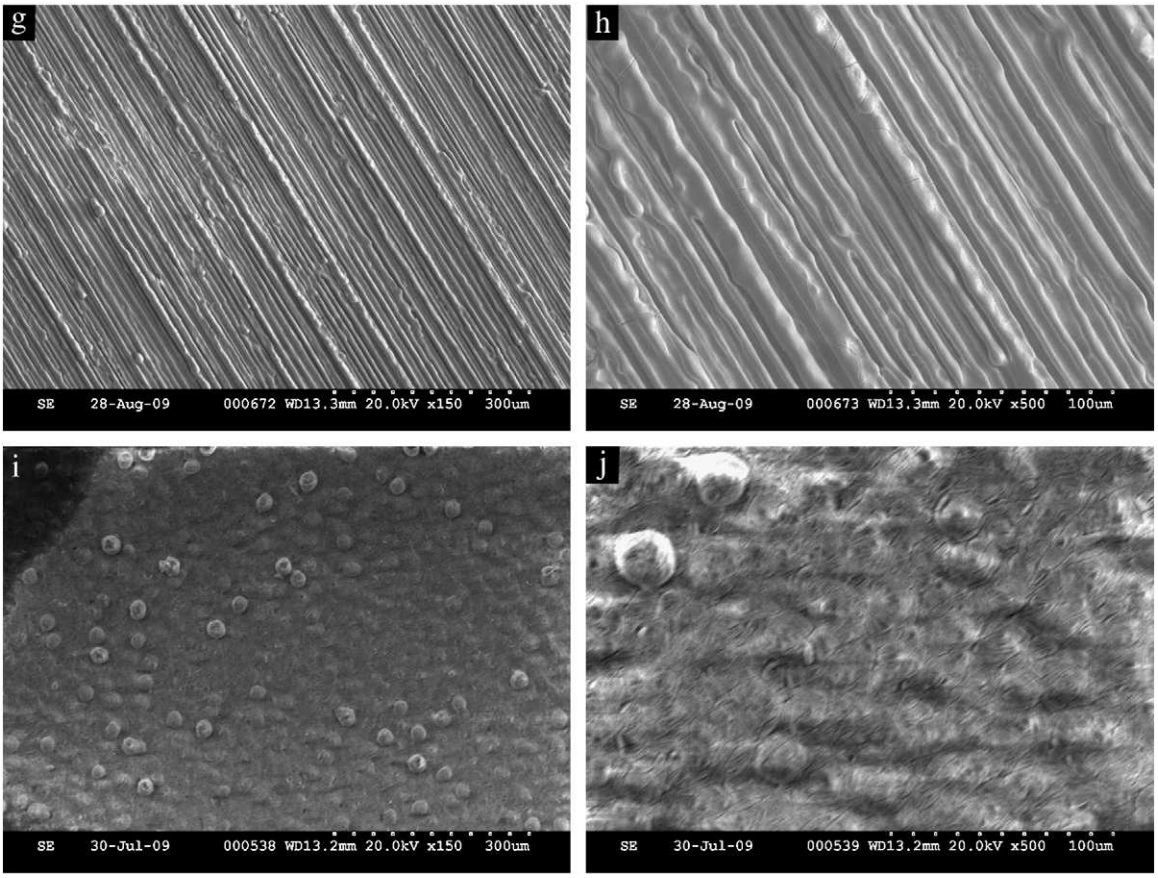

Fig. 1 (*continued*).

3. Results and discussion

3.1. Characterization of ceramic coatings on P91 prepared by spray pyrolysis deposition

XRD spectra of the coatings indicate that the as-deposited coatings are basically amorphous after heat treatment at 600 °C. This is in agreement with the results from other researchers [15,16]. According to the studies of thermogravimetric analysis (TGA) on the same precursor with the similar processes, the precursor has completely decomposed after a heat treatment at 600 °C [17]. Fig. 1 shows the SEM images of the top surfaces of the coatings. The coatings with different compositions show various morphologies due to the diverse behaviour of nucleation and growth of the oxide materials. The coatings were dense but there are some shallow micro-cracks on the top of some of the Al_2O_3 coatings (Fig. 1a and b). The coatings were gradually built up during the deposition by the repeated movement of the spray nozzle. Due to the repetitive nature of the process, when shallow micro-cracks form on top of a coating during a spray run, the next run would fill the cracks. Therefore, such shallow micro-cracks were not a problem for obtaining dense coatings. The thickness of as-deposited oxide coatings is 2–5 μm, as listed in Table 2.

Oxidation is a common corrosion mechanism for many alloys in SCW environments [5]. We studied the effect of these coatings on the corrosion properties of P91 exposed to supercritical water at 500 °C and 25 MPa with a dissolved oxygen concentration below 20 μg/kg for exposure times up to 500 h. As shown in Fig. 2, the weight changes due to the oxidation and corrosion of P91 with the coatings are all smaller than that observed on the bare P91 alloy with the exception of the S3 coupons (CeO_2–Ta_2O_5 coating), which showed a similar weight gain to blank P91. The S4 coupons (ZrO_2–MgO coating) seemed to reduce the overall weight gain on the P91 by a factor of 2 while all the coupons coated with alumina (Al_2O_3 – coupons S1, S2 and S5) exhibited weight losses as opposed to weight gains. Further, the deposition technique seems to play a role since the higher pH precursor solution (S2 coupons) and the PSD + ESD techniques (S5 coupons) showed very little weight loss over the 500 h of exposure while the S1 coupons seemed to be losing weight, most likely due to loss of the Al_2O_3 surface coating. This is somewhat verified by examination of the surfaces of each of these samples after the supercritical water exposure. Fig. 3 (a–f) shows the cross-sectional SEM images of the S1, S2 and S5 samples before and after the 500 h of exposure. Clear and well-bonded interfaces between the substrates

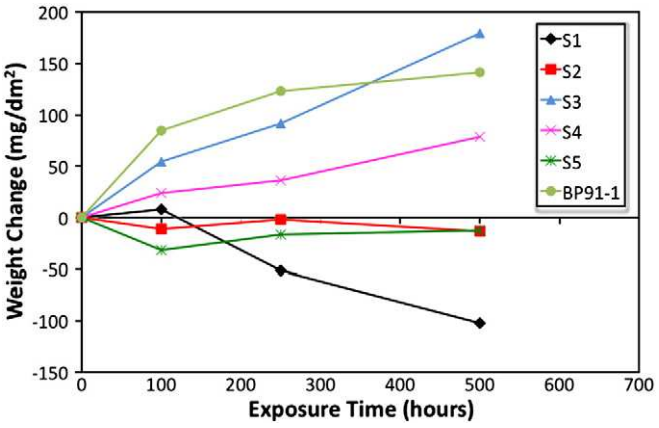

Fig. 2. Weight gain versus time for the blank P91 substrate (BP91-1) and P91 with different coatings prepared by spray pyrolysis method: (S1) Al_2O_3; (S2) Al_2O_3; (S3) CeO_2–Ta_2O_5; (S4) ZrO_2–MgO; and (S5) Al_2O_3, and exposed to supercritical water at 500 °C, 25 MPa, and DO<20 ppb.

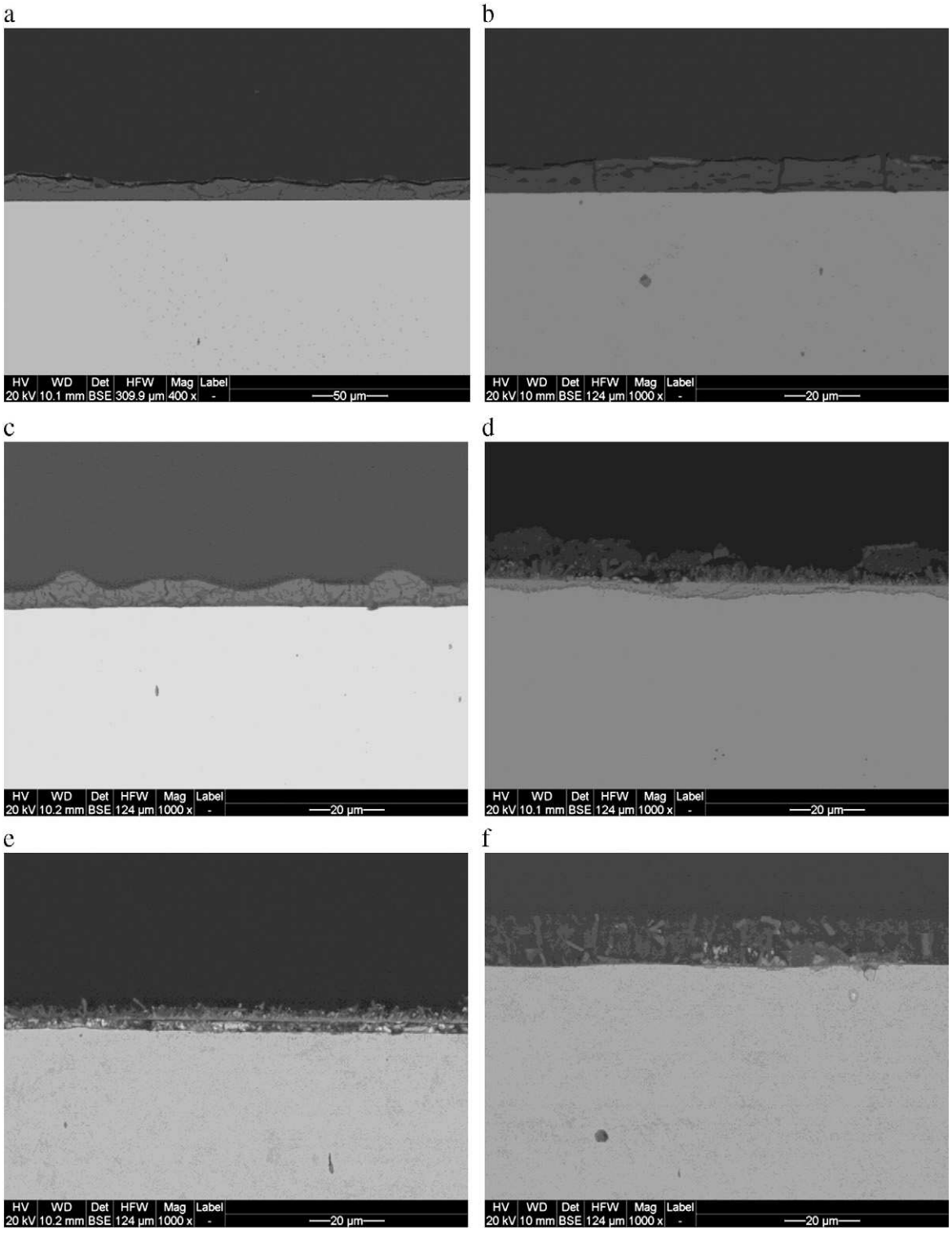

Fig. 3. Cross-sectional SEM images of samples S1, S2 and S3 pre-exposure (a–c) and post-exposure (d–f) to supercritical water at 500 °C, 25 MPa and DO<20 ppb.

and the coatings could be observed. The SEM observation was consistent with the result from scratch adhesion testing made on the same coatings. In the testing, a Rockwell C diamond scratching indenter could not induce interface failure between the coating and the substrate at a normal load of 50 N. As can be seen when comparing the unexposed samples to the exposed samples with the same preparation techniques, there is more prominent dissolution and breakdown of the alumina film on the S1 samples than on the S2 and S5 ones. The Al_2O_3 coatings on the S2 and S5 samples are altered from their pre-exposure morphology, potentially due to dissolution of the ingredients in the coating and their re-precipitation.

To evaluate the stability of the alumina coatings under the supercritical water conditions, theoretical calculations based on the Gibbs Free Energy of reaction can provide significant insight into the potential causes of oxide dissolution and breakdown. The details of the calculation methods can be found elsewhere [18,19], but the method is based on evaluating the free energy of formation of the pure materials and dissolved species using the revised Helgeson–Kirkham–

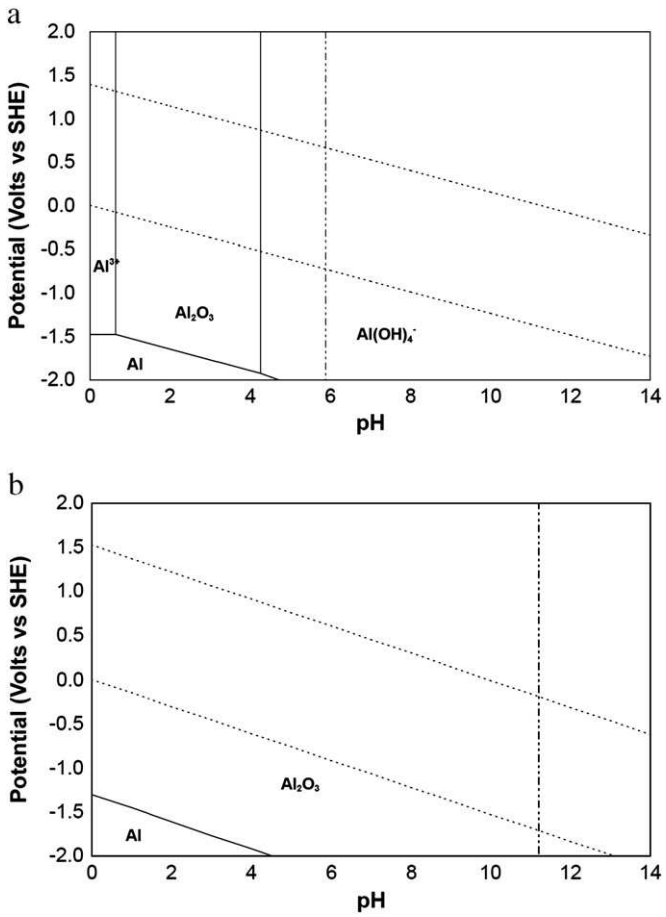

Fig. 4. Pourbaix diagrams for Al/Al_2O_3–water system at 25 MPa and (a) 350 °C at 10^{-6} mol/kg, (b) 500 °C at 10^{-8} mol/kg.

Flowers (HKF) model to extrapolate the required thermodynamic properties to the temperatures and pressures of interest. Once these values are obtained, Pourbaix diagrams may be constructed and the solubility of the oxides of interest calculated using equilibrium equations and overall solution charge balances. This procedure was carried out for alumina and the results are presented in Fig. 4 (a and b) and Fig. 5.

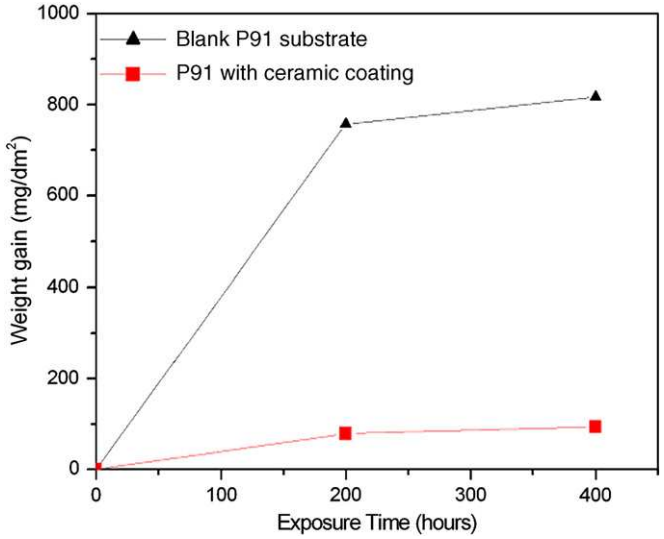

Fig. 6. Weight gain versus time for the blank P91 substrate and P91 with an Al_2O_3 coating prepared by spray pyrolysis (as sample S1) and exposed to supercritical water at 650 °C, 25 MPa, and with dissolved oxygen concentration < 2 μg/kg in a static autoclave.

Fig. 4 (a and b) shows the Pourbaix diagrams constructed for the aluminum/alumina system under sub-critical (350 °C) and supercritical (500 °C) water conditions at 10^{-6} and 10^{-8} mol/kg concentrations, respectively. The dotted vertical lines on the diagram represent the neutral point of water under the given conditions, as this is the chemistry relevant to the present tests. As can be seen, under supercritical conditions (Fig. 4b) the only stable species present is alumina over virtually the entire pH range covered on the diagram. No soluble species are found to be present in the Pourbaix diagrams until the concentration at which the diagram is constructed is lowered significantly – down to 10^{-15} mol/kg (note, this diagram is not shown here). This shows that alumina is insoluble under the supercritical water conditions. The situation is much different in the sub-critical solution. The Pourbaix diagram presented in Fig. 4a shows that at 350 °C and neutral conditions, a soluble species ($Al(OH)_4^-$) is the stable species, even at concentrations as high as 10^{-6} mol/kg. The overall solubility of alumina in neutral water from sub-critical to supercritical conditions has been calculated and is shown in Fig. 5. What the combination of these diagrams show is a significant solubility for the alumina coating at temperatures below the critical

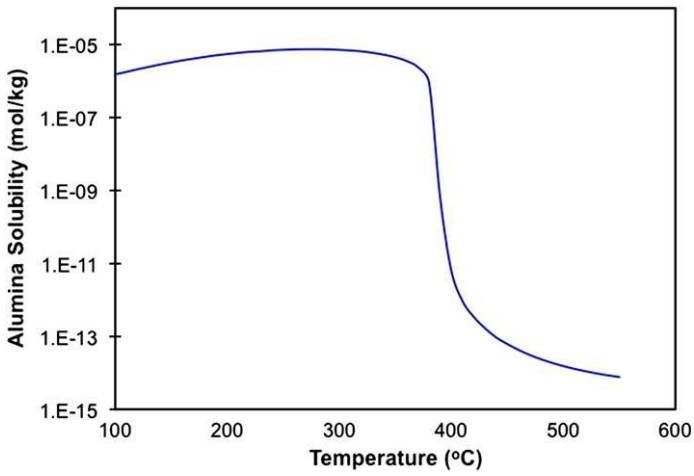

Fig. 5. Theoretical solubility of Al_2O_3 in sub-critical and supercritical water at 25 MPa under neutral conditions.

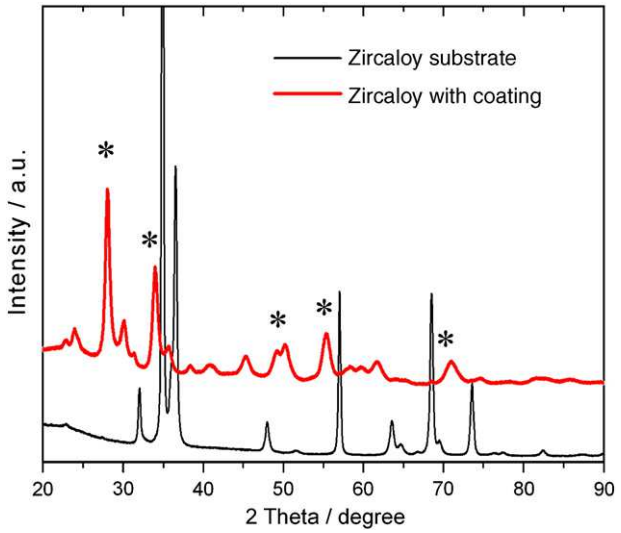

Fig. 7. XRD patterns of the Zr–2.5Nb substrate and the coated sample (*ZrO_2 peaks).

point and a very insoluble and stable alumina coating above the critical point. This helps to explain the apparent dissolution, breakdown and re-crystallization of the coatings shown in the cross-sectional SEM images in Fig. 3, where ramping the temperature of the test loop up to operational temperature at the beginning of the tests and cooling during the frequent shut-downs to remove the samples has had significant effects on the structure of the coatings. This might also explain the presence of cerium and tantalum in some of the coatings on the S2 series coupons as a carryover from the S3 samples – although this is solely speculation at this point.

P91 samples with the Al_2O_3 coating prepared using the same conditions as those of samples S1 above were also tested at Shanghai JiaoTong University at a higher temperature and lower DO concentration. As shown in Fig. 6, the weight gain of the coated P91 sample is about eight times less than that of the uncoated sample during a 400 h static autoclave test at 650 °C and 25 MPa with less than 2 μg/kg DO present. This result indicates that P91 with an Al_2O_3 coating has superior resistance at higher temperatures in SCW environment and can act to significantly protect the P91 substrate in high-temperature supercritical water. As shown in Fig. 2, the Al_2O_3 coatings existed in the state of amorphous phase after deposition at 600 °C. It is not clear if the amorphous phase have superior corrosion resistance over the crystallized phases under supercritical water conditions. This needs to be studied through phase comparison in the future.

3.2. Characterization of coatings on Zr–2.5Nb prepared by plasma electrolytic oxidation

The phases of the coating material were characterized by XRD for sample S6 – Zr–2.5Nb samples. Fig. 7 shows the XRD patterns of the Zr–2.5Nb samples with and without the coating. In contrast to the XRD patterns obtained from the Zr–2.5Nb substrate, the main phase of sample with the coating is Baddeleyite-type ZrO_2 (JCPDS no. 37-1484). No peaks from the substrate were observed on the coated sample. This is a good indication that the PEO coating formed on the Zr–2.5Nb substrates is thick and crack-free.

Fig. 8 (a and b) shows the surface of the coating prepared at 2700 Hz, $D = 20\%$, and $R = 3$. It can be seen that, at these magnifications, the coating appears no open pores and virtually crack-free. Fig. 8 (c and d) shows cross-sectional SEM images of the coating and show that the coating is continuous and uniform (Fig. 8c). From the high-

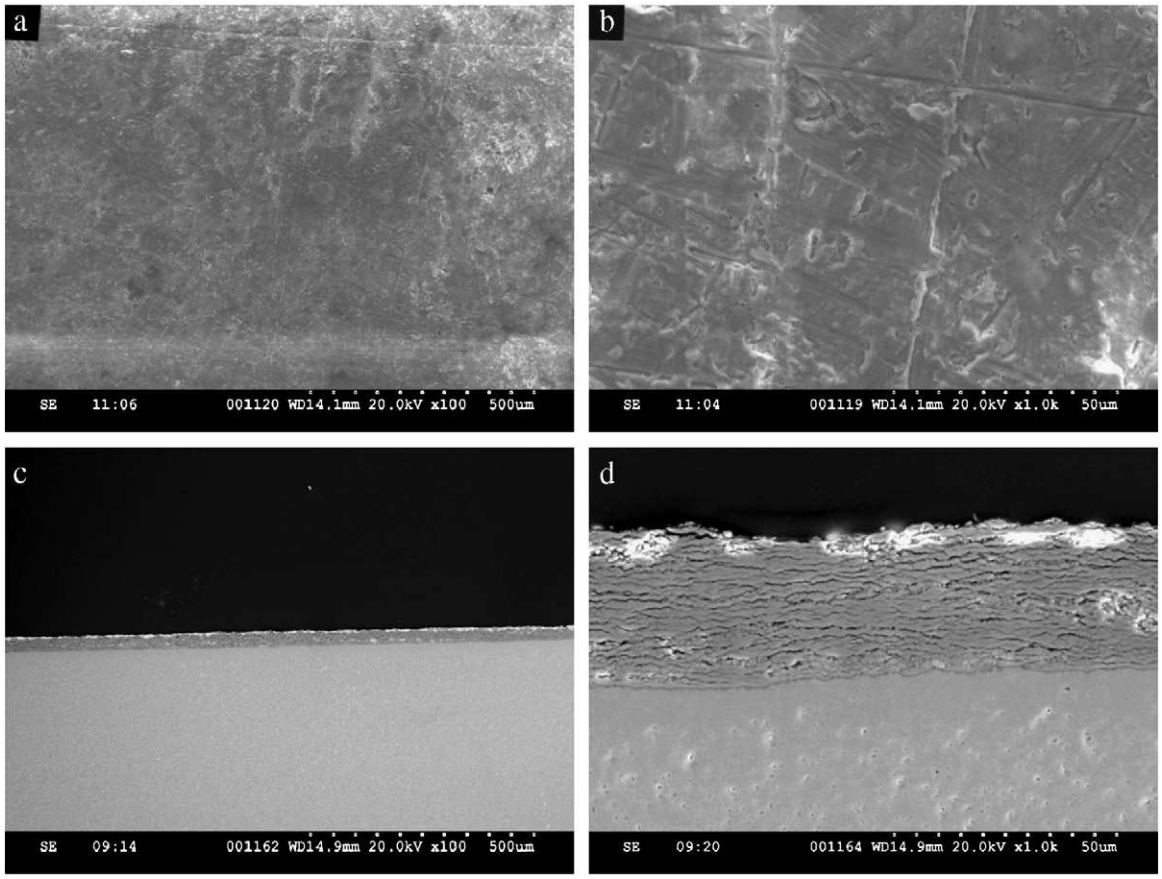

Fig. 8. Surface SEM images (a, b) and cross-sectional SEM images (c, d) of the coatings formed on Zircaloy by plasma electrolytic oxidation.

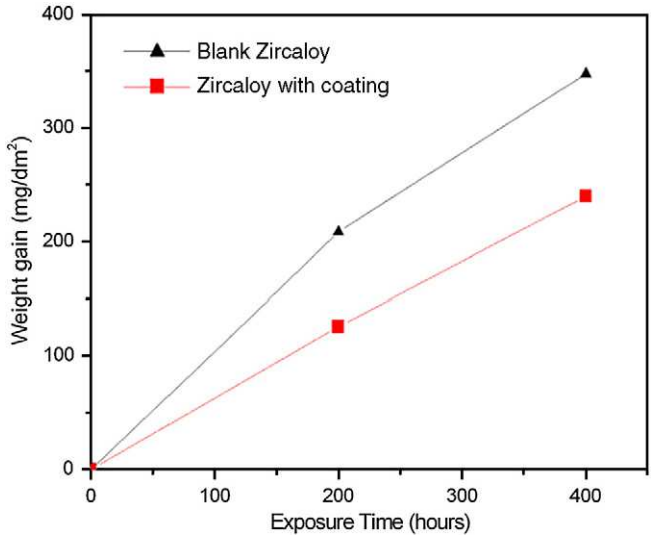

Fig. 9. Weight gain versus time for the Zirc–2.5Nb substrate with and without coatings prepared by plasma electrolytic oxidation and exposed to supercritical water at 500 °C, 25 MPa, and DO concentration <5 ppb in a static autoclave at Shanghai JiaoTong University.

magnification SEM image (Fig. 8d), it can be seen that the coating is composed of a multi-layered structure, which suggests that the deposit grows layer by layer on the surface as the electrolytic process proceeds. The total thickness of the as-deposited ZrO_2 oxide coating is about 30 μm. The thickness of a single layer is about 1–2 μm.

The corrosion resistance of the coated Zircaloy was studied by exposing the samples to supercritical water at 500 °C and 25 MPa with a DO concentration below 5 μg/kg at Shanghai JiaoTong University in a static autoclave. As shown in Fig. 9, the weight gain due to oxidation of the coated Zr–2.5Nb sample is about 1.5 times less than that of uncoated Zircaloy coupon for exposure times up to 400 h in the Shanghai tests. However, tests show a value for the weight gain – between 200 and 350 mg/dm^2, which are considered too high for use in actual supercritical water applications and further improvement of the coating properties are required in the future.

4. Conclusions

Thin and dense ceramic oxide coatings have been deposited by spray pyrolysis on P91 substrates as protective coatings. At 500 °C and 25 MPa, and DO concentration <20 μg/kg in a flow loop, Al_2O_3 coatings were stable and effective in preventing substantial oxidation of the substrate in a supercritical water environment while coatings based on MgO–ZrO_2 and CeO_2–Ta_2O_5 were considerably less effective. A P91 substrate with a Al_2O_3 coating is thought to be a promising candidate material for SCWR out-core applications, however in sub-critical water the Al_2O_3 coatings appear to be quite soluble. This effect need considerably more study as a reactor will be in a sub-critical state quite often during start-up and shut-down operations. Further studies will involve the characterization of the microstructure of the coatings and the optimisation of the coating thickness to ensure sufficient corrosion resistance under the expected SCW environment. A metallic bond coating will also be designed which would be applied on the bare substrate prior to the spray pyrolysis process in order to improve the thermal-mechanical compatibility between the P91 alloy and the alumina top coat.

ZrO_2 coatings without open pores and crack-free were formed successfully on Zr–2.5Nb substrates using a plasma electrolytic oxidation method. The coated Zr–2.5Nb samples showed somewhat better corrosion resistance than the bare substrates when tested in static autoclaves but showed more-or-less identical weight changes when tests in a flowing system. Further studies will focus on systematically evaluating the effects of processing parameters and electrolyte solution on the microstructures and the resistance to corrosion under supercritical water conditions. The demonstrated superior corrosion-resistant properties of P91 with Al_2O_3 ceramic coatings in SCW environments compared with those of pristine substrates suggests that this process has application potential in the development of SCW reactors.

Acknowledgment

The authors acknowledge the financial support from the Canadian National Program on Generation IV Energy Technologies, the NSERC/NRCan/AECL Generation IV Technologies Program and the CANMET-MTL REIM program for invaluable help on the microstructure characterization using SEM.

References

[1] U.S. DOE Nuclear Energy Research Advisory Committee and the Generation IV International Forum, A Technology Roadmap for Generation IV Nuclear Energy Systems, 2002http://gif.inel.gov/roadmap/pdfs/gen_iv_roadmap.pdf.
[2] G. Gupta, P. Ampornrat, X. Ren, K. Sridharan, T.R. Allen, G.S. Was, J. Nucl. Mater. 361 (2007) 160.
[3] Y. Chen, K. Sridharan, T. Allen, Corros. Sci. 48 (2006) 2843.
[4] P. Kritzer, N. Boukis, E. Dinjus, J. Supercri, Fluids 5 (1999) 205.
[5] C.W. Sun, R. Hui, W. Qu, S. Yick, Corros. Sci. 51 (2009) 2508.
[6] K. Ehrlich, J. Konys, L. Heikinheimo, J. Nucl. Mater. 327 (2004) 140.
[7] N. Hara, K. Sugimoto, Mater. Jpn. 39 (2000) 325.
[8] N. Boukis, N. Claussen, K. Ebert, R. Janssen, M. Schacht, J. Eur. Ceram. Soc. 17 (1997) 71.
[9] P.S. Patil, Mater. Chem. Phys. 59 (1999) 185.
[10] Y. Xie, R. Neagu, C.S. Hsu, X. Zhang, C. Decès-Petit, W. Qu, R. Hui, S. Yick, M. Robertson, R. Maric, D. Ghosh, J. Fuel Cell Sci. Technol. 7 (2) (2010) 021007.
[11] A.L. Yerokhin, X. Nie, A. Leyland, A. Matthews, S.J. Dowey, Coat. Technol. 122 (1999) 73.
[12] E. Matykina, P. Skeldon, G.E. Thompson, Surf. Eng. 23 (2007) 412.
[13] J. Sun, W. Qian, W. Qu, S. Hui, PCT/CA2010/000987, "Novel pulsed power supply for plasma electrolytic deposition and other processes", filed 06/08/2010.
[14] C. Sun, R. Hui, W. Qu, S. Yick, C. Sun, W. Qian, J. Mater. Sci. 45 (2010) 6235.
[15] M. Aguilar-Frutis, J. Guzmán-Mendoza1, T. Alejos1, M. García-Hipólito, C. Falcony, Phys. Stat. Sol. (A) 199 (No. 2) (2003) 227.
[16] N. Bahlawane, Thin Solid Films 396 (1–2) (2001) 126.
[17] B. Pacewska, M. Keshr, Thermochim. Acta 385 (2002) 73.
[18] W.G. Cook, R.P. Olive, 2nd Canada-China Joint Workshop on Supercritical Water-Cooled Reactors, Toronto, April 2010.
[19] W.G. Cook, R.P. Olive, NPC2010, Quebec City, October 2010.